forests

MDPI

Article

Effects of Long-Term Subculture on Maturation Ability and Plant Conversion in *Pinus radiata*: Using FT-IR Spectroscopy to Determine Biomarkers of Embryogenic Tissue Aging

Yenny Lineros [1,2,3,*], Macarena Rojas-Rioseco [4,5], Martha Hernández [2], Darcy Ríos [2], Ximena Muñoz [1] and Rodrigo Hasbún [3,*]

1 Investigaciones Forestales Bioforest S.A., Unidad de Biotecnología, Camino a Coronel km 15, Concepción 4190000, Chile; ximena.munoz@arauco.com
2 Laboratorio de Cultivo de Tejidos Vegetales, Facultad de Ciencias Forestales y Centro de Biotecnología, Universidad de Concepción, Victoria 631, Concepción 40730386, Chile; marhernandez@udec.cl (M.H.); drios@udec.cl (D.R.)
3 Laboratorio de Epigenética Vegetal, Departamento de Silvicultura, Facultad de Ciencias Forestales, Universidad de Concepción, Victoria 631, Concepción 40730386, Chile
4 Laboratorio de Bioespectroscopia y Quimiometría, Centro de Biotecnología, Universidad de Concepción, Victoria 631, Concepción 40730386, Chile; macarrojas@udec.cl
5 Departamento de Análisis Instrumental, Facultad de Farmacia, Universidad de Concepción, Concepción 4070386, Chile
* Correspondence: yenny.lineros@arauco.com (Y.L.); rodrigohasbun@udec.cl (R.H.)

Abstract: The forestry industry has integrated somatic embryogenesis into its clonal programs due to the generation of a high number of plants from selected genotypes at low cost. Somatic embryos are generated in a stressful environment after multiplication of the proembryogenic masses; thus, it is critical to determine the degree of stability of the embryogenic cultures and their potential for mass propagation. Maturation ability in cultures of different ages was evaluated in conjunction with the integrity of the proembryogenic masses, germination rate, hypocotyl and root length, plant conversion, and ex vitro survival. To identify differences in embryogenic tissue from different subcultures, their DNA was analyzed using FT-IR spectroscopy. A significant decrease in the production of somatic embryos was detected from week 15, and some lines even stopped producing embryos. Germination rate, hypocotyl length, and plant conversion were negatively affected by long-term cultivation, while root length and ex vitro survival were not significantly affected. The results obtained from the FT-IR spectroscopy analysis indicate that it is feasible to use mid-infrared spectroscopy to differentiate between embryogenic tissues with different cumulative subculture times based on the spectra obtained from their DNA, which is directly related to maturation ability.

Keywords: radiata pine; somatic embryogenesis; proliferation; somatic embryos; mid-infrared

Citation: Lineros, Y.; Rojas-Rioseco, M.; Hernández, M.; Ríos, D.; Muñoz, X.; Hasbún, R. Effects of Long-Term Subculture on Maturation Ability and Plant Conversion in *Pinus radiata*: Using FT-IR Spectroscopy to Determine Biomarkers of Embryogenic Tissue Aging. *Forests* **2023**, *14*, 1446. https://doi.org/10.3390/f14071446

Academic Editors: Marcos Edel Martinez-Montero and Judit Dobránszki

Received: 9 June 2023
Revised: 3 July 2023
Accepted: 6 July 2023
Published: 14 July 2023

1. Introduction

In Chile, forest plantations cover an approximate area of 2.3 million hectares, of which 55.5% comprise *Pinus radiata*. The main reasons why *P. radiata* is selected to establish forest plantations are due to its high rusticity, easy management in plantations, and rapid growth when established in appropriate climates and soils [1,2], as well as the versatility of its wood [3]. In order to establish highly productive plantations, the Chilean national forestry industry has chosen to integrate biotechnological tools, such as plant tissue culture, into its breeding programs to optimize the generation of a high number of plants of selected genotypes at a low cost.

Somatic embryogenesis (SE) is one of the most promising tissue culture biotechnological tools for large-scale vegetative propagation of woody plants of economic value, being considered the most effective method for the mass propagation of different *Pinus*

species [4–6]. In *P. radiata* and in other conifers, its application allows the vegetative production of genetic material in breeding programs and in clonal forestry at an operational scale [7,8]. The success of SE depends on many factors, such as the nature of the explant, the microenvironment generated by the in vitro culture conditions, and the regulation of gene expression, among others [9]. For the formation and development of the somatic embryos (*Se*), complex cellular, biochemical, and molecular processes are required [10]. To activate these processes in the explant, it is necessary to apply specific conditions such as stress (mechanical, osmotic, chemical, heavy metals, hypoxia, temperature, and ultraviolet light), as well as specific levels of endogenous and exogenous plant growth regulators (PGRs) [11].

The most widely used plant growth regulator (PGR) to induce SE and maintain cell proliferation is the exogenous auxin 2.4-Dichlorophenoxyacetic acid (2.4-D) [12]. Its incorporation into the embryogenic cultures under different conditions (endogenous or exogenous to the explant) can influence metabolic patterns, gene expression, and epigenetic mechanisms of the explant (such as DNA methylation, histone modifications, and microRNAs), causing a cell (or a group of cells) to change its course [13]. It has been reported that high concentrations or long exposure times to auxins, especially 2.4-D, can block the normal development of the *Se*, altering the balance of endogenous auxins and the polar transport of auxins and interfering with the apical-basal polarity of the embryo [14,15].

In most conifers, the multiplication of the proembryogenic masses (PEMs) that give rise to *Se* remains constant for years without any notable change in the multiplication rate or maturation ability (MA). However, reports indicate that in pine species, the situation is quite different. It has been observed that the yields in maturation and the length of the *Se* decrease as a function of the number (and time) of subcultures [16–20]. In addition, morphological degradation prevents the formation of early embryos, indicating a global loss of MA, which may be increased by manipulation during subculture [21]. These results shed light on the biochemical effects of in vitro cultures as well as the deleterious effects of age on them. All these findings adhere to the concept of cell line aging, which would indicate that cells begin to transform into recalcitrant cells as ET accumulates subculture time [22,23].

Problems surrounding this process make it difficult to propagate plants on a large scale by SE in *Pinus* species since production costs are increased by the lack of a priori knowledge of whether the genotypes being propagated have lost their MA. From the point of view of the mass production of plants, it would be desirable to have some biomarker that would indicate whether ET has the capacity to generate *Se*. Nowadays, there are traditional techniques, such as transcriptomics [24], proteomics [25], and metabolomics [26], that could allow the determination of molecular markers in order to differentiate the state of a tissue. Biomarkers of SE in *Pinus* species may include polyamines and their biosynthetic enzymes [27], gene transcripts involved in embryogenesis and maturation [28], and proteins related to somatic embryo maturation [29]. Specifically, one study of *Pinus pinaster* identified changes in the expression levels of specific genes during the maturation process [30]. However, further research is needed to confirm and expand on these findings.

Vibrational spectroscopic techniques like Fourier transform-infrared spectroscopy (FT-IR) have proven their potential to provide information on the structural and chemical changes in tissues or cells in a simple, fast, and inexpensive way [31–33]. The changes in the type, conformation, or number of bonds produce different spectra that can be used to distinguish tissues with different characteristics. [34,35]. Previously, FT-IR was used by Bravo et al. [36] to determine differences between cell lines previously characterized in terms of their embryogenic potential in *P. radiata*.

The objective of this study was to determine the effect of long-term subculture of the embryogenic tissue on the loss of maturation ability and plant conversion and to evaluate the applicability of FT-IR spectroscopy to determine biomarkers of the maturation ability of embryogenic tissues in *Pinus radiata*.

2. Materials and Methods

2.1. Plant Material

Immature *P. radiata* cones were collected from a controlled crossing orchard located in the Bío-Bío region of Chile and belonging to the ARAUCO company. Following collection, the cones were stored at 4 °C in perforated polyethylene bags until processing. Disinfection was carried out by immersing them in a 10% (v/v) hydrogen peroxide solution for 5 min. Next, they were rinsed three times with sterile distilled water in order to extract their seeds. Afterwards, the seeds were manually extracted and placed in sterile petri dishes for a maximum of 24 h at 4 °C. They were then sterilized in a laminar flow cabinet by immersing them in 10% (v/v) hydrogen peroxide for 5 min. Finally, they were rinsed three times with sterile distilled water [7].

2.2. Embryogenic Culture Induction and Proembryogenic Mass Proliferation

The sterilized seeds were deposited without their coating in 94 × 16 mm Petri dishes with 30 mL of modified semi-solid Litvay medium (mLM) [37]. The culture medium was supplemented with 4.5 µM 2.4-Dichlorophenoxyacetic acid (2.4-D), 2.7 µM 6-benzylaminopurine (BAP), 30 g L^{-1} sucrose, and 3 g L^{-1} Phytagel®. The pH was adjusted to 5.6 before autoclaving at 121 °C and 1 ATM pressure. After 12 weeks in culture, the seeds that presented friable cell proliferation were transferred to an individual Petri dish with fresh culture medium [7].

The same culture medium used in induction was used in ET multiplication. The culture was changed to a fresh medium every 7 days, for a total period of 66 weeks. The subculture was carried out in a combined manner. First, in agglomerates of approximately 1 cm in diameter, and then in cell suspensions dispensed on filter paper deposited in a semi-solid medium. The embryogenic material was kept in dark conditions at 23 ± 1 °C.

To determine the embryogenic potential of the cell lines obtained, preparations of 20 mg of fresh ET were made. A total of 10 µL of 2% (w/v) acetocarmine stain was added for 4 min to the ET, followed by two washes with distilled water. The stained tissue was placed on a slide covered with a coverslip and observed with a Carl Zeiss Axiostar Plus light microscope. Embryonic lines were considered those with the presence of the three types of PEMs described by Filonova et al. [23].

2.3. Cryopreservation and Recovery

For the cryopreservation of ET, the slow freezing protocol described by Hargreaves et al. [38] was used, with some modifications. Seven days after the last subculture and approximately 6 to 10 weeks after induction, ET was resuspended in 11 mL of liquid multiplication mLM. First, ET was pretreated for 48 h with 0.4 M sorbitol in orbital agitation at 80 rpm under dark conditions at 23 ± 1 °C. Following this, 10 aliquots of 5% (v/v) Dimethyl sulfoxide (DMSO) were applied. Furthermore, 1.5 mL aliquots of this suspension were dispensed into 2 mL Nalgene cryovials, which were stored in Mr. Frosty Nalgene containers in a −80 °C freezer for 120 min. Finally, the cryovials were immersed in liquid nitrogen (−196 °C) for approximately 5 weeks.

For ET thawing, the cryovials were immersed in sterile water at 37 °C for 1 to 2 min. They were then externally disinfected with 70% (v/v) ethanol. To reactivate the growth of the cryopreserved tissue, the content of each cryovial was placed on a filter paper (Fisher Scientific, grade P5, Waltham, MA, USA). Finally, the filter was placed in a Petri dish with proliferation mLM. The culture media changes were performed weekly for 1 month. A positive control was used, which contained ET with the addition of cryoprotectants but without immersion in liquid nitrogen. This was in order to rule out a negative effect from the chemicals used as cryoprotectants.

2.4. Maturation

The maturation was carried out 10 days after the last subculture in the multiplication phase. ET was resuspended in falcon-type tubes with liquid maturation culture medium. Subsequently, the tissue was dispensed onto filter paper in mLM supplemented with

90 µM abscisic acid, 60 g L^{-1} sucrose, and 10 g L^{-1} Phytagel®. A concentration of 80 mg of tissue per Petri dish was used. ET was selected in the proliferation phase with different accumulated subculture times and was transferred to the maturation phase. The following treatments were considered, depending on the time in the proliferation phase (letter C indicates cryopreservation, and the number indicates the number of weeks on proliferation medium after growth reactivation of cryopreserved lines): C0: non-cryopreserved tissue; C + 4: ET at 4 weeks; C + 7: ET at 7 weeks; C + 12: ET at 12 weeks; C + 15: ET at 15 weeks; C + 22: ET at 22 weeks; C + 26: ET at 26 weeks; C + 34: ET at 34 weeks; C + 44: ET at 44 weeks; C + 59: ET at 59 weeks; C + 66: ET at 66 weeks. The treatments were categorized, according to the accumulated subculture time, as young (C0), middle (C + 4), and aged (from C + 15).

Embryogenic cell line tissue was incubated for 5 months until the complete maturation of the embryos in dark conditions at a temperature of 23 ± 1 °C. To determine the ability to differentiate PEMs into cotyledonary *Se* (maturation ability), the number of cotyledonary *Se* per gram of fresh weight of ET (N° *Se*/g FW) was counted. Depending on the maturation ability (productivity), the embryogenic lines were classified as low, medium, and high.

2.5. Germination and Plant Conversion

Germination and conversion to plants of the *Se* obtained were evaluated for three different accumulated subculture times. C0: non-cryopreserved tissue (young); C + 4: ET at 4 weeks (middle); and C + 34: ET at 34 weeks (aged). Since the negative effects of prolonged subcultures were observed from week 15, we considered evaluating germination and conversion to plants at an earlier time (34 weeks) and not waiting until the final period of 66 weeks, where some genotypes did not generate *Se*. The *Se* with normal morphology (opaque, white coloration, and three or more well-developed cotyledons) were put to germinate. Germination was carried out in 200-milliliter polypropylene containers with modified Pullman No. 55 medium [39]. The germination medium was supplemented with 20 g L^{-1} sucrose, 0.6 g L^{-1} activated carbon g L^{-1}, and 4 g L^{-1} Phytagel®. The embryos were germinated horizontally in Petri dishes at an inclination of 45° at 23 ± 1 °C. A 16-h photoperiod with a light intensity of 10 µmol m^{-2} s^{-1} was used during the first week of culture. They were then cultured between 40 and 70 µmol m^{-2} s^{-1} for 10 weeks.

After thirty days, the percentage of germinated *Se* was evaluated. At 45 days, the average length of the hypocotyl and root of the emblings was evaluated. The same light intensity was used for the emblings elongation. Once the emblings were established under ex vitro conditions, their survival at 30 days was assessed.

2.6. FT-IR Microspectroscopy and Multivariate Analysis

Before maturation, samples of ET from three embryogenic lines were taken at different subculture times to extract DNA, using the protocol proposed by Bravo et al. [36]. The analyzed samples were categorized, according to the accumulated subculture time, as young (C0), middle (C + 4), and aged (C + 66). Of each sample, 50 µL of DNA (200 ng) were dried in Mirr IR reflective glass (Kevey Technologies, Chesterland, OH, USA) in the dark to prevent photo and atmospheric oxidation. All FT-IR spectral acquisitions of dried DNA pellets were performed in the absorption mode, from 4000 to 500 cm^{-1}, using a Spotlight 400 imaging system spectrophotometer (Perkin Elmer, Middlesex, MA, USA) equipped with a Duet™ design detector containing a nitrogen-cooled MCT detector and a linear array MCT imaging detector. For each DNA sample, 20 scans of 100 × 100 µm were taken, providing a spectral resolution of 2 cm^{-1}.

2.6.1. Spectral Pretreatment

Once the spectra were acquired, the spectral region of interest between 1800 and 700 cm^{-1} was selected. Furthermore, a second spectral derivative with a window of 11 points, using the Savitzky-Golay algorithm and mean centering, was applied for trans-

formation and preprocessing, respectively. The pretreatments and analyses were performed using PLS-Toolbox (Eigenvector Research, Inc., Manson, WA, USA).

2.6.2. Multivariate Analysis

Principal Component Analysis (PCA)

The exploratory analysis of data allows for the detection of atypical samples as well as observation of the behavior of the samples (e.g., clustering) through the decomposition of the original matrix (X) into matrices of scores (T), loadings (P), and residuals (E) (Equation (1)).

$$X = TP^T + E \quad (1)$$

Two PCAs were carried out to analyze (i) young, middle, and aged samples and (ii) young samples only. Scores and loading plots were evaluated to analyze the behavior of the samples and identify the most influential bands, respectively. PLS-Toolbox (Eigenvector Research, Inc., Manson, WA USA) software was used.

Supervised Classification Method

As a supervised pattern recognition method, Partial Least Squares—Discriminant Analysis (PLS-DA) was applied. PLS-DA is a multivariate supervised dimensionality reduction tool, unlike PCA. This classification method is based on the Partial Least Squares Regression (PLS-R) algorithm, except that the response variable is categorical [40–42]. Using the PLS-Toolbox (Eigenvector Research, Inc.) software, two PLS-DA models were built for three (young, middle, and aged) and two classes (young and aged). The confusion matrix, classification error rate, and variable importance in projection (VIP) were evaluated.

2.7. Statistical Analysis

The experiment was carried out with a completely randomized design. MA was tested in 21 genotypes in three biological replicates with five Petri dishes at 11 different times of accumulated subculture. For germination, hypocotyl and root length, and plant conversion, five genotypes in three replicates at three different times of accumulated subculture were analyzed: C0, C + 4, and C + 34. Mean values were expressed with standard error, and the significant differences were tested by one-way ANOVA analysis of variance followed by Tukey's multiple analysis test at $p \leq 0.05$. The data were analyzed with InfoStat software (v.2008). For FT-IR analysis, 3 genotypes were evaluated at 3 different times of accumulated subculture: C0 (young), C + 4 (middle), and C + 66 (aged). The multivariate analysis is detailed in Section 2.6.2.

3. Results

3.1. Maturation Ability of Short-Term Subcultured Embryogenic Tissue

The maturation ability of the studied embryogenic lines was significantly affected by the genotype ($p \leq 0.05$). Only *Se* with normal characteristics were counted. We considered normal *Se* those who presented 3 or more cotyledons completely developed, white-yellow coloration, and a good proportion of shape. The genotypes were classified according to their productivity: 23.8% with low productivity, 52.4% with medium productivity, and 23.8% with high productivity. The least productive genotype was L8529, with 23 *Se*/g FW, while MH102 was the most productive, at 400 *Se*/g FW (Table 1). In general, all the genotypes tested presented a response to maturation to a lesser or greater extent, observing an asynchrony in the development of the *Se*, which is usually observed in *P. radiata*.

Table 1. Mean number of somatic embryos per gram of fresh weight (N° *Se*/g FW) of 21 *Pinus radiata* genotypes before cryopreservation, classified according to their productivity. Different letters indicate significant differences according to Tukey's test ($p < 0.05$).

Genotype	Maturation Ability (Productivity)	N° *Se*/g FW
L8529	Low	23 ± 2.4 a
M101		33 ± 6.0 a
L8521		36 ± 2.1 ab
M108		38 ± 2.6 ab
M106		45 ± 2.0 abc
M263	Medium	75 ± 5.5 bcd
L8510		81 ± 7.3 cde
M103		88 ± 2.7 def
M137		93 ± 7.1 def
M100		119 ± 8.3 efg
MH114		124 ± 5.5 fg
G228		125 ± 5.5 fgh
MH124		125 ± 4.9 fgh
M130		138 ± 9.4 gh
M123		143 ± 10.2 gh
M102		164 ± 3.0 hi
MH111	High	200 ± 16.3 i
H409		258 ± 15.7 j
MH122		302 ± 10.0 k
MI101		317 ± 6.3 k
MH102		400 ± 22.0 l

3.2. Long-Term Subcultured Embryogenic Tissue Characterization

After cryopreservation, ET did not present macromorphological differences until the final evaluation period (66 weeks). All the embryogenic lines presented a good proliferation rate and were friable and whitish in color during the entire culture period (Figure 1A). Therefore, to corroborate the good morphological state of the ET studied and to identify the presence of PEMs, microscopic observations were made 66 weeks after having been maintained in the proliferation phase. For all the genotypes, the presence of PEMs was consistent, indicating that the ET condition was maintained despite the long time in culture. Type I PEMs were composed of a small group of meristematic cells with a prominent nucleus and dense cytoplasm, accompanied by 1 or 2 highly vacuolated, small-nucleated suspender cells (Figure 1B). Type II PEMs were observed to have a similar appearance but with a greater number of grouped meristematic and vacuolated cells (Figure 1C). Type III PEMs were larger in size, with many embryogenic cells being observed, forming a highly dense central conglomerate surrounded by suspensor cells. In addition to this cluster, the presence of early proembryos could be observed in some genotypes (Figure 1D).

Figure 1. Embryogenic tissue (ET) and proembryogenic masses (PEMs) were observed after the long-term proliferation phase for 66 weeks. (**A**) ET clusters on proliferation; (**B**) PEM type I; (**C**) PEM type II; (**D**) PEM type III. The black arrow indicates early somatic embryo formation in type III PEM. ESE: early somatic embryo; MC: meristematic cells; SC: suspensor cells. Bar = 200 µm.

3.3. Maturation Ability of Long-Term Subcultured Embryogenic Tissue

The relationship between MA and age (accumulated time in the proliferation phase) of ET was inversely proportional. In Figure 2, it is observed that the mean number of cotyledonary *Se* for all genotypes tested from young tissue without cryopreservation (C0) was 139.4 *Se*/g FW. The MA of the ET 4 weeks after its post-cryopreservation reactivation of growth (C + 4) decreased by 5.9% in relation to the value obtained in the ET without cryopreservation (C0). From week 7 (C + 7) and up to week 12 (C + 12), a significant increase in MA of 26.8% and 33.4%, respectively, was observed. The most abrupt change was observed in week 15 (C + 15), where it decreased by 17.8% in relation to the control (C0). From this time onward, a tendency towards decreased generation of *Se* was observed as the ET continued to be maintained in subculture in the proliferation phase. From week 34 (C + 34), a stabilization in the MA was observed until week 66 (C + 66). At this cumulative subculture time, the loss of MA was 47.9% with respect to its basal value (C0), and some of the lines studied no longer produced embryos. For the three conditions evaluated, no differences were observed in terms of the morphology of mature embryos.

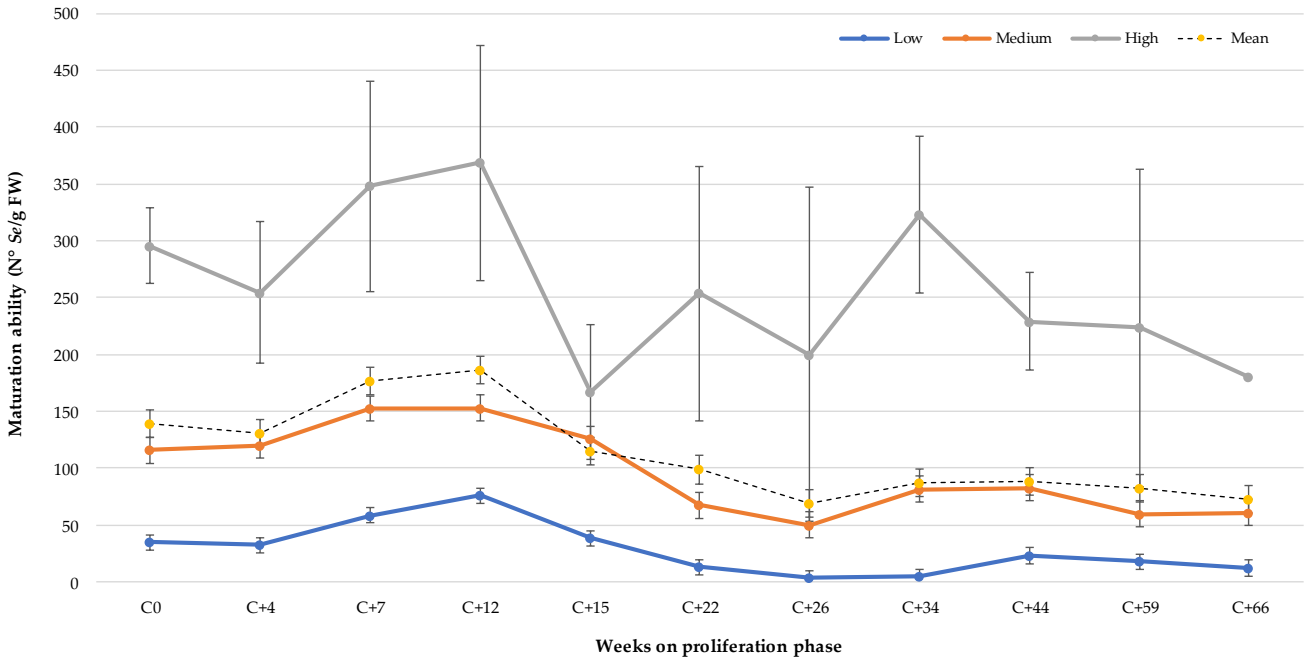

Figure 2. Maturation ability (N° *Se* g/FW) of *Pinus radiata* embryogenic lines with different productivity at different times in the post-cryopreservation proliferation phase (C0 represents the number of *Se* before cryopreservation).

A grouping of genotypes by productivity was carried out due to the considerable differences observed between genotypes with respect to their MA (Table 1). Similar behavior was observed for all groups with regard to the trend of genotypes with low, medium, and high productivity, with the latter demonstrating the most abrupt changes due to the magnitude of the number of *Se*/g FW. In the high and low productivity genotypes, there was a decrease in MA at week 4 (C + 4), while the average productivity value remained similar. For the three classification groups, the maximum MA was recorded at 12 weeks of subculture after growth reactivation. On average, the high productivity genotypes presented a 38.9% decrease at 66 weeks of subculture (C + 66) in their MA in relation to the non-cryopreserved ET (C0), while those of medium and low productivity had a loss of 47.3% and 65.1%, respectively (Figure 2). These results show that the lower the productivity of the embryogenic lines, the greater the loss of MA as the subculture time increases in the proliferation phase.

3.4. Morphological Characterization of Plant Conversion Originating from Young and Aged Embryogenic Tissue

After 30 days of *Se* germination, the differences were significant between young, middle, and aged ET (Figure 3). The subculture time of the ET showed a negative correlation with the germination rate of *Se*, where germination decreased up to 34.7% in *Se* from aged tissue in relation to young tissue. For the three evaluated conditions, *Se* with normal morphology without germination were observed in similar quantities; however, a higher number of abnormal *Se* with signs of oxidation were observed in aged tissue, which presented a brown coloration, necrosis, and malformations.

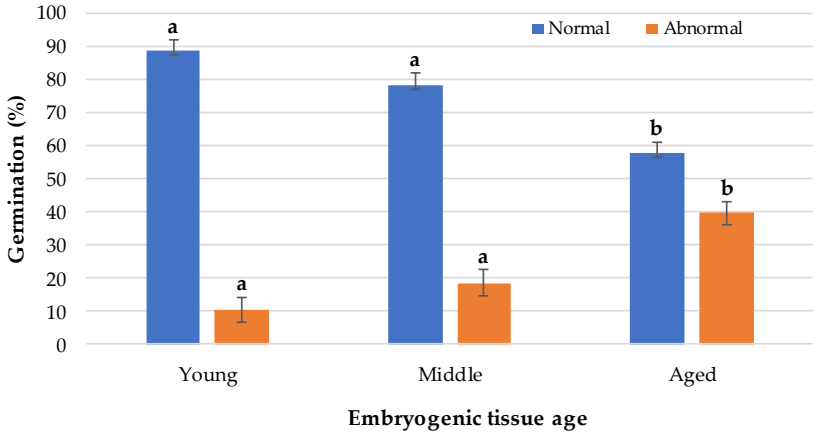

Figure 3. Germination of somatic embryos from embryogenic tissue of different ages. Different letters indicate significant differences according to Tukey's test ($p < 0.05$).

After 45 days of *Se* germination, those from younger tissue presented similar morphologies, showing good development of the hypocotyl and its roots. Most showed apical development and green coloration without signs of oxidation. On the other hand, the length of the hypocotyl was affected in the embryos from older tissue (Figure 4A), and in general, they presented a later apical development than those from young tissue, although they did not present significant differences in the length of their roots (Figure 4B).

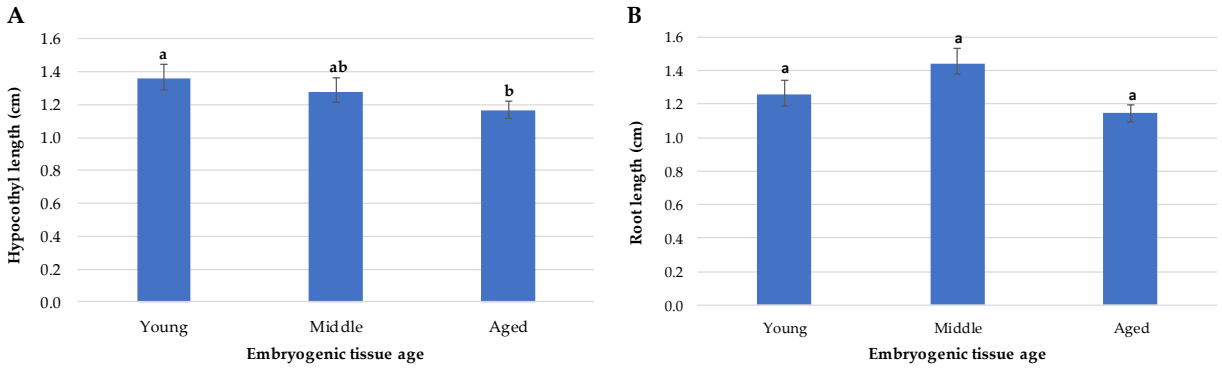

Figure 4. Morphological characteristics of 45-day emblings from embryogenic tissue of different ages. (**A**) Average hypocotyl length. (**B**) Average root length. Different letters indicate significant differences according to Tukey's test ($p < 0.05$).

The germinated embryos were changed every 30 days to fresh culture medium, eliminating those emblings that had not presented apical development at the second subculture or had died. Once the emblings grew to 1.5 to 2 cm in length, they were sent to a greenhouse with controlled temperature and humidity conditions and constant mist irrigation. The percentage of dispatched plants was calculated in relation to the germinated plants with normal growth. No significant differences were observed regarding the conversion to

plants of *Se* from juvenile ET (C0 and C + 4), where 60% and 61.6% were obtained, respectively. The emblings from aged tissue with characteristics of being dispatched ex vitro decreased considerably, to only 33.3% (Figure 5A). Once the emblings were established in the greenhouse, survival at 30 days of acclimatization was evaluated, and no significant differences were observed. The observed survival values remained above 70%, which is expected for the environmental conditions to which the emblings were exposed (Figure 5B). Once the emblings reached 10 cm in length, they were kept under sprinkler irrigation, and the light intensity was increased.

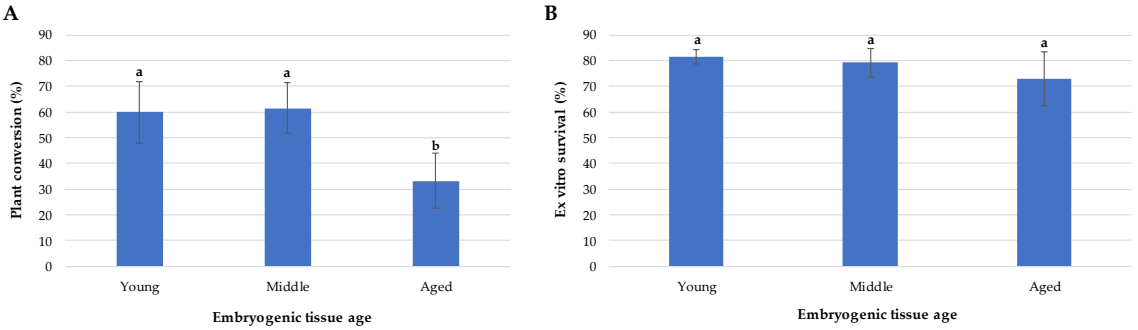

Figure 5. Plant conversion. (**A**) Average percentage of emblings shipped to the greenhouse. (**B**) Average percentage of ex vitro survival of the emblings at 30 days. Different letters indicate significant differences according to Tukey´s test ($p < 0.05$).

3.5. DNA Infrared Spectroscopy

To provide visualization of the differences in the absorption maxima, the raw mean FT-IR spectra are shown in Figure 6A, with each spectrum colored according to age. Contrasting samples from young (C0), middle (C + 4), and aged (C + 66) ET were used for this analysis. The bands between 1800 and 700 cm^{-1} were selected, where each band represents an average of three biological replicates for each condition. In this region, we can find vibrational changes associated with nucleic acids that can provide important information about the behavior of the ET DNA with different accumulated subculture times, depending on the specific place where these variations are found.

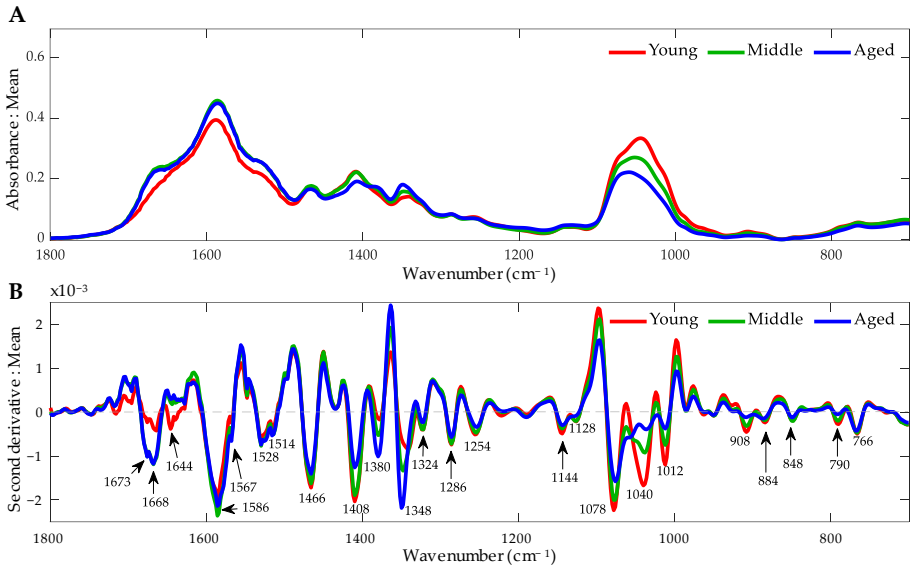

Figure 6. FT-IR spectra of embryogenic tissue of *Pinus radiata* DNA from the fingerprint zone (1800 to 700 cm^{-1}) under different age conditions. (**A**) Average raw FT-IR spectrum. (**B**) Average second derivative spectrum. Arrows indicate the main bands.

However, given the overlapping that characterizes this spectral zone, the second derivative of the average spectra of each class was observed, identifying those bands that differ in their absorption maxima (Figure 6B). In this way, it is observed that there are multiple bands that differ according to the class. This mathematical procedure was carried out to avoid the problem of overlapping bands and to suppress the constant background noise. In this way, it was possible to improve the resolution of the spectrum, facilitating the interpretation of the data obtained.

3.5.1. Principal Component Analysis

In the PCA analysis, according to the time in subculture, it was possible to observe that PC1 (explained by 41.77% of the variance) separates the young samples from the old ones (Figure 7A), with the middle sample in between the two. On the other hand, a separation of genotype 1 is observed in relation to genotype 2 and genotype 3 in the young and middle samples. However, in the aged samples, this separation is not clearly observed. Figure 7B shows the loading plot, in which the four most important variables are highlighted: the bands at 1350 and 1100 cm^{-1} are associated with young samples, and the bands at 1080, 1040, and 1364 cm^{-1} are associated with aged samples.

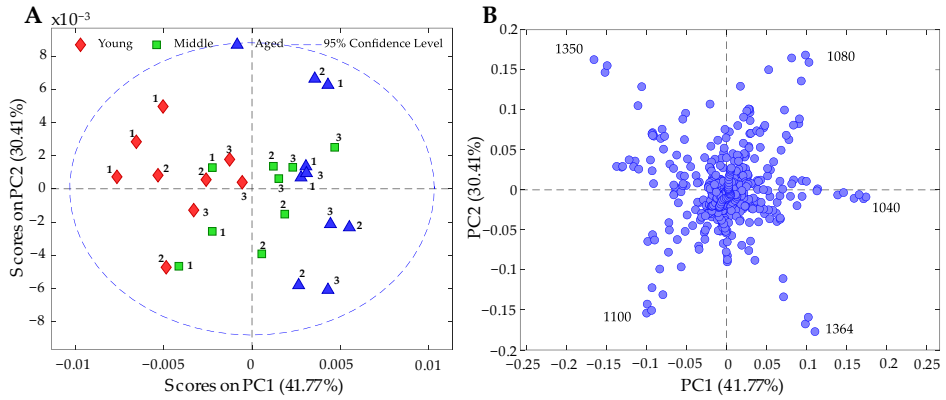

Figure 7. PCA results of FT-IR spectral data on genomic DNA according to condition (young, middle, and aged). (**A**) Score plot of PC1 vs. PC2, explaining 72.18% of the variance. The numbers represent genotypes 1, 2, and 3. (**B**) Loading plot of PC1 vs. PC2; the most important bands are shown.

As already observed, the middle samples were not separated by any principal component; therefore, a PCA was carried out only for the classes of young and aged (Figure 8A). PC1, which explains 51.50% of the variance, separates the samples of these conditions into two clusters.

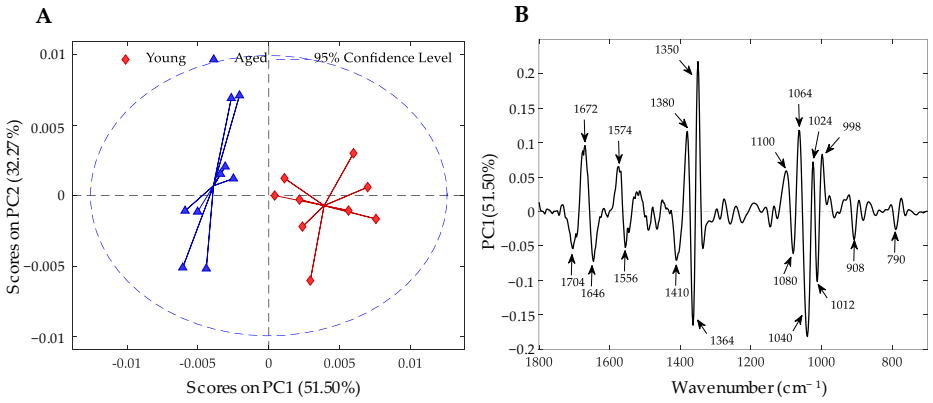

Figure 8. PCA results of FT-IR spectral data on genomic DNA according to condition (young and aged). (**A**) Scores plot of PC1 vs. PC2, explaining 83.77%. (**B**) Loading plot of PC1; the most important bands are shown. Variables with positive values are important wavenumbers for young samples, and those with negative values are important for aged samples.

Regarding the loading plots (Figure 8B), it was possible to identify the variables that are important for each condition. The variables with positive values for PC1 are important bands for the young samples; among them, the bands at 1672, 1574, 1380, 1350, 1100, 1064, 1024, and 998 cm^{-1} are the most outstanding. On the other hand, for the aged samples, the most important variables are observed with negative values for PC1, such as the bands at 1704, 1646, 1556, 1410, 1364, 1336, 1080, 1040, 1012, 908, and 790 cm^{-1}.

3.5.2. Classification Method According to Condition

As observed in the exploratory analysis, the samples according to genotype do not present any pattern that would allow observing clustering; therefore, this was not modeled for classification. On the contrary, PLS-DA classification models were built to classify the samples according to their condition. The results of the cross-validation for the two models are presented in Table 2. The model developed between the three conditions did not give good classifications, achieving 70.4% classification accuracy. As already seen in the PCA (Figure 7A), the middle samples were between the young and aged samples, so a poor classification was to be expected. On the other hand, when the model was built only for young and aged samples, the classification accuracy increased considerably, to 100%.

Table 2. Cross-validation confusion matrices for the classification between young-middle-aged and young-aged samples using the PLS-DA model. Y: young; M: middle; A: aged; %CA: percentage of classification accuracy (% of samples correctly classified).

Classes	**PLS-DA**				
Young-Middle-Aged	Actual class	Predicted as class			%CA
		Y	M	A	
	Y	7	2	0	77.8
	M	3	5	1	55.6
	A	0	2	7	77.8
		Mean			70.4
Young-Aged	Actual class	Predicted as class			%CA
		Y		A	
	Y	9		0	100.0
	A	0		9	100.0
		Mean			100.0

Thus, it is possible to correctly classify *Pinus radiata* DNA samples according to their condition as young or aged; we can also associate certain bands with this classification. This can be seen in the variable importance in projection (VIP) plot (Figure 9). Among the most important bands to differentiate and distinguish both conditions are the bands at 1350 and 1040 cm^{-1}. Furthermore, all the bands above the significance threshold lie in the observed bands on the loading plot (Figure 8B). By analyzing both graphs together, it was possible to identify which bands were significant for each condition. This is summarized in Table 3.

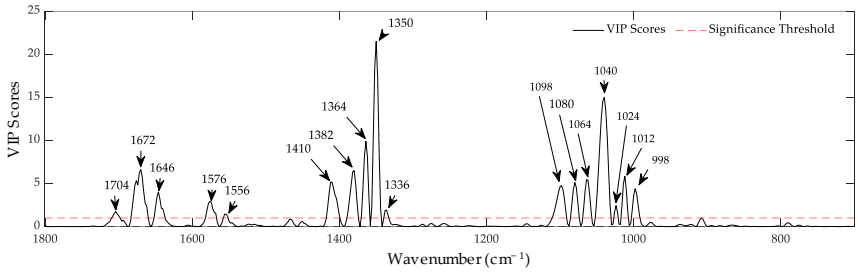

Figure 9. Variable importance in projection (VIP) plot of the PLS-DA model according to young-aged condition. The bands above the significance threshold are the most important for classification.

Table 3. Important information for each class of the most relevant bands identified by the VIP (PLS-DA) and loading (PCA) plots.

Wavenumber (cm^{-1})		Associated to the Class
PCA	**VIP**	
1704	1704	Aged
1672	1672	Young
1646	1646	Aged
1574	1576	Young
1556	1556	Aged
1410	1410	Aged
1380	1382	Young
1364	1364	Aged
1350	1350	Young
1336	1336	Aged
1100	1098	Young
1080	1080	Aged
1064	1064	Young
1040	1040	Aged
1024	1024	Young
1012	1012	Aged
998	998	Young

4. Discussion

Determining how to reduce costs in the SE process without affecting the quality of the embryos is an issue facing many companies and institutions that promote SE, in combination with cryopreservation, as a vital biotechnological tool in clonal forestry [22,43] and genomic selection [44,45]. In addition to improving methods for PEMs induction, *Se* differentiation, germination, and emblings conversion, it is important to connect these steps effectively to maximize production efficiency and minimize economic cost [46,47]. SE requires complex cellular, biochemical, and molecular processes for embryo formation and development. Thus, in order to use SE as a complement to clonal forestry, it is essential to determine the degree of stability of the crop yield due to the accumulated effects in all in vitro stages [48].

The effect of prolonged subculture of coniferous ET has been widely reported, and the most affected species seem to be of the genus *Pinus*. It has been observed that as ET enters its active proliferative phase, increasing its growth rate, disorganization is generated in the cellular structures that compose it, indicating progressive aging [16]. In our study, this disorganization caused a substantial loss in MA, consistent with what was observed in other species, such as *Pinus pinaster*, *Pinus massoniana*, *Pinus koraiensis*, and *Picea balfouriana* [19,21,48,49], where a degradation of immature embryos was also observed, depending on the number of accumulated subcultures. This degradation, resulting from the presence of numerous suspensor cells, likely affects developmental signaling within the embryo, which implies a certain degree of recalcitrance in pine species and is associated with the events that govern the initial formation of the suspensor [15].

To date, there have been different theories on the possible mechanisms associated with the loss of yield in the maturation phase, in addition to the damage that could be generated because of handling during subculturing. Although, in some species, ET can multiply in culture media free of PGRs [50], the vast majority require a complex network of interactions between endogenous and exogenous PGRs, mainly auxins and cytokinins, during the early pro-embryogenic stages and ethylene, gibberellic, and abscisic acids later in the development of *Se* [11,51,52]. Therefore, prolonged exposure to these regulators, mainly 2.4-D auxin, could generate an imbalance in their transport or synthesis, which could cause problems in the following stages [14,19,53].

An important and still suboptimal process during in vitro *Se* maturation is the biosynthesis and deposition of storage proteins, which are rich in high-nitrogen (N) amino acids

such as arginine. The mobilization of these N-rich proteins is essential for the germination and production of vigorous somatic seedlings [54]. Although low conversion to plants has been reported in some conifers, this has been associated with specific genotypes [55]. In the data obtained, the lower germination rate observed in *Se*, the decrease in hypocotyl length, and the low conversion to plants were observed in all genotypes, indicating a cross-sectional effect resulting from ET aging. This effect has been reported in other mass-produced species, such as *Coffea arabica* [56] and *Olea europaea* [57]. On the other hand, in these species, as in our study, no differences were observed in rooting, survival, or ex vitro acclimatization for the generated emblings.

The results obtained indicate that there may be large losses of productivity (MA) because of the time of subculture, even reaching losses of over 60% in lines maintained for more than 1 year. Although, in general terms, it has been described that the reduction of the MA in species of the genus *Pinus* can occur in about 9 months [22], in our laboratory, we observed that for *Pinus radiata*, this time could be shorter and was consistent for embryogenic lines with different degrees of productivity (low, medium, and high). In a previous work carried out by our work team, we observed that after cryopreservation there was a decrease in the MA [7]; however, on that occasion, this parameter was only evaluated 4 weeks after growth reactivation, which coincides with the data obtained in this study (C + 4). In this study, where the evaluation was carried out for a later and longer time, it was observed that the young ET can improve its MA as a result of a potential beneficial effect of cryopreservation, similar to what was reported in white spruce by Gao et al. [58]. This is because the genes involved in stress response and auxin signal transduction could promote the expression of genes associated with the development of early *Se* [59] or the elimination of non-embryogenic cells with a high water content, which favors the development of viable meristematic cells in the embryo head. Therefore, considering the number of subcultures prior to cryopreservation (8 weeks on average) and the decrease in MA observed beginning at 15 weeks post-cryopreservation (C + 15), it is notable that after 6 months of proliferation, ET begins a considerable decrease in the production of *Se*.

The main problem is that the decline or loss of MA is only visible after maturation. *Se* maturation is one of the longest and most expensive phases of SE [60], and for this reason, it is necessary to ensure that the ET used is in optimal conditions to generate the *Se* that will give rise to the plants. As a result of long-term storage of embryogenic cultures, loss of embryogenic potential and maturation ability has been reported due to the accumulation of somaclonal variations as a result of changes in the level of ploidy, gene mutations, and/or changes in DNA methylation levels [61]. In studies on the somaclonal variation associated with the age of the cultures, the observed effects have a predominance only in some specific genotypes [62], and in other cases, they are associated with abnormal *Se* phenotypes at the precotyledon and cotyledon level [63], which could suggest that some embryogenic lines could be more susceptible as they get older. In studies where 5-azacitidine (5-azaC) has been applied to aged ET, it has been shown that the methylation pattern can be manipulated by treating the cultures with this hypomethylating drug since the observed response was an increase in fresh mass and the potential for *Se* maturation [64]. It has been reported that DNA methylation is higher in those lines that are not highly productive in terms of *Se* generation [17,65]. Although these evaluations were not carried out on the same genotypes over time, this could suggest that epigenetic effects may play an important role in the correct development of *Se* as the ET ages. Although this information does address the root cause of the problem, it could guide us towards the use of tools to identify this problem at an early stage through rapid DNA analysis. In this way, it would be possible to identify the ET that is still capable of generating *Se* and generate work strategies that allow maximizing the use of ET when undertaking mass production of plants in clonal forestry programs.

A technique that allows us to identify changes at the global level of DNA is FT-IR spectroscopy [31]. This technique uses mid-infrared radiation to detect the vibration of certain molecular groups present in biological samples. According to Tymchenko et al. [66], the fingerprint region can be divided into three different spectral zones for DNA: the

1800–1550 cm^{-1} region is mainly represented by the absorption of groups in the nitrogenous bases of DNA. This region is characterized mainly by vibrations of the C=O, C=N, and C=C bonds of purine and pyrimidic DNA rings [67,68]. The 1550–1160 cm^{-1} region mainly comprises the vibrations of groups within bases and sugars of DNA. This region is characterized mainly by C3′-endo sugar vibrations [69] and by vibrations of the C=N bonds of adenine and guanine [66]. The 1150–800 cm^{-1} region represents the vibrations of groups within the sugar-phosphate backbone of DNA. This region is characterized mainly by symmetric PO_2- vibrations, diester bond vibrations, and deoxyribose vibrations [70]. The analysis of the DNA spectra from young and aged *Pinus radiata* ET shows differences in these three regions in a large number of bands, which could be used as markers of ET age to predict MA.

The double helical structure of DNA, which is stabilized by long-range intra- and inter-backbone forces, including hydrogen bonds between base pairs and stacking interactions between neighboring bases, may exist in different conformations [71]. The four most important bands were chemically assigned; the bands assigned to young tissue were the bands 1672 cm^{-1} and 1350 cm^{-1}, which were associated with C=O stretching of guanine and with purine in syn conformation, respectively [72,73]. The bands assigned to aged tissue were the bands 1364 cm^{-1} and 1040 cm^{-1}, which were associated with cytidine in anti-conformation and with C-O stretching vibrations of the backbone, respectively [72,74].

Multivariate analysis allowed us to identify the characteristic peaks in the spectra that are responsible for the greatest variation between an ET capable of generating *Se* (young) and one that has lost its MA (aged). The results of our work indicate that it is possible to discriminate between embryogenic tissue DNA samples with different cumulative subculture times, which in turn is related to the MA of each of them. Although the analysis does not show a clear separation of genotypes in samples with different subculture times, it is interesting to observe that in young samples, it is possible to discriminate a genotype of low productivity (genotype 1) from a medium one (genotype 3) and a good one (genotype 3). This needs to be validated with a greater number of genotypes in future studies. This find would also be very useful since it could allow the identification of genotypes with low or high maturation abilities prior to entering them into the maturation phase, which is one of the most expensive phases in the plant production process through somatic embryogenesis. With this, genetic materials with good probabilities of generating *Se* could be selected at an early stage, which would decrease the costs of plant production.

5. Conclusions

The prolonged subculture of *P. radiata* ET generates losses in maturation ability in the medium term. Therefore, for the use of SE in clonal forestry, it is critical to determine the degree of stability of crop yield in addition to the potential for mass propagation. The morphological aspects that have been analyzed in this study in relation to the decrease in the MA of the *Pinus radiata* ET subcultured in the long term give us a vision of the importance of generating cultivation strategies, combined with cryopreservation, which can ensure the mass propagation of elite genotype plants.

Given that the macromorphological aspect and, in some cases, the microscopic observations of the ET do not indicate abnormalities that could indicate a loss of the tissue's ability to generate mature *Se* that will give rise to emblings, it is necessary to have other quality predictors. The results obtained from the FT-IR spectroscopy analysis indicate that it is feasible to use mid-infrared spectroscopy to differentiate between ETs with different cumulative subculture times based on the spectra obtained from their DNA, which is directly related to maturation ability.

Our results are intended to support the search for quality control tools that will allow SE to be a profitable technique as a large-scale plant production system. More studies are required to simplify the sampling of ET and evaluate the consistency of this predictor across a large number of genotypes.

Author Contributions: Conceptualization, Y.L., M.R.-R., M.H., D.R., X.M. and R.H.; conducting of experiments, Y.L.; methodology, Y.L. and M.R.-R.; formal analysis, Y.L., M.R.-R., M.H., D.R. and R.H.; writing—draft preparation, Y.L., M.R.-R. and R.H.; writing—review and editing, Y.L., M.R.-R., M.H., D.R., X.M. and R.H.; supervision, M.H. and R.H.; project administration, Y.L. and R.H.; funding acquisition, Y.L. and X.M. All authors have read and agreed to the published version of the manuscript.

Funding: This research received no external funding.

Data Availability Statement: The data presented in this study are available on request from the corresponding author. The data are not publicly available due to privacy.

Acknowledgments: The authors would like to thank the Chilean National Agency for Research and Development (Agencia Nacional de Investigación y Desarrollo de Chile, ANID) for the doctoral scholarship ANID-Subdirección de Capital Humano/Doctorado Nacional/2022-21220260 in support of the lead author (Y.L.). The authors wish to express their thanks to ARAUCO (Investigaciones Forestales Bioforest S.A) for their role in providing the plant material and financial support for this study. Special thanks to Mónica Guiñez for her support in carrying out the laboratory experiments.

Conflicts of Interest: The authors declare no conflict of interest.

Abbreviations:

SE: Somatic embryogenesis; *Se*: Somatic embryos; PGRs: Plant growth regulators; ET: Embryogenic tissue; 2.4-D: 2.4-Dichlorophenoxyacetic acid; PEMs: Proembryogenic masses; MA: Maturation ability; FT-IR: Fourier transform-infrared spectroscopy; mLV: Modified semi-solid Litvay medium; DMSO: Dimethyl sulfoxide; PCA: Principal component analysis; PLS-DA: Partial least squares discriminant analysis; PLS-R: Partial least squares regression; VIP: Variable importance in projection.

References

1. Álvarez, V.; Poblete, P.; Soto, D.; Gysling, J.; Kahler, C.; Pardo, E.; Bañados, J.C.; Baeza, D. *Anuario Forestal*; INFOR: Santiago, Chile, 2022; 262p. [CrossRef]
2. Watt, M.S.; Palmer, D.J.; Kimberley, M.O.; Höck, B.K.; Payn, T.W.; Lowe, D.J. Development of models to predict *Pinus radiata* productivity throughout New Zealand. *Can. J. For. Res.* **2010**, *40*, 488–499. [CrossRef]
3. Bayne, K.M. Wood Quality Considerations for Radiata Pine in International Markets. *N. Z. J. For.* **2015**, *59*, 23–31.
4. Salaj, T.; Klubicová, K.; Matusova, R.; Salaj, J. Somatic Embryogenesis in Selected Conifer Trees *Pinus nigra* Arn. and *Abies* Hybrids. *Front. Plant Sci.* **2019**, *10*, 13. [CrossRef]
5. Reeves, C.; Tikkinen, M.; Aronen, T.; Krajnakova, J. Application of Cold Storage and Short In Vitro Germination for Somatic Embryos of *Pinus radiata* and *P. sylvestris*. *Plants* **2023**, *12*, 2095. [CrossRef]
6. Castander-Olarieta, A.; Moncaleán, P.; Montalbán, I. Somatic Embryogenesis in Pines. *Methods Mol. Biol.* **2022**, *2527*, 41–56. [CrossRef] [PubMed]
7. Lineros, Y.; Balocchi, C.; Muñoz, X.; Sánchez, M.; Ríos, D. Cryopreservation of *Pinus radiata* embryogenic tissue: Effects of cryoprotective pretreatments on maturation ability. *Plant Cell Tissue Organ Cult.* **2018**, *135*, 357–366. [CrossRef]
8. Hazubska-Przybyl, T.; Bojarczuk, K. Tree Somatic Embryogenesis in Science and Forestry. *Dendrobiology* **2016**, *76*, 105–116. [CrossRef]
9. De-la-Peña, C.; Nic-Can, G.I.; Galaz-Ávalos, R.M.; Avilez-Montalvo, R.; Loyola-Vargas, V.M. The role of chromatin modifications in somatic embryogenesis in plants. *Front. Plant Sci.* **2015**, *6*, 635. [CrossRef]
10. Us-Camas, R.; Rivera-Solís, G.; Duarte-Aké, F.; De la Peña, C. In vitro culture: An epigenetic challenge for plants. *Plant Cell Tissue Organ Cult.* **2014**, *118*, 187–201. [CrossRef]
11. Fehér, A. Somatic embryogenesis—Stress-induced remodeling of plant cell fate. *Biochim. Biophys. Acta* **2015**, *1849*, 385–402. [CrossRef]
12. Karami, O.; Aghavaisi, B.; Mahmoudi Pour, A. Molecular aspects of somatic-to-embryogenic transition in plants. *J. Chem. Biol.* **2009**, *2*, 177–190. [CrossRef]
13. Osorio-Montalvo, P.; Sáenz-Carbonell, L.; De-la-Peña, C. 5-Azacytidine: A Promoter of Epigenetic Changes in the Quest to Improve Plant Somatic Embryogenesis. *Int. J. Mol. Sci.* **2018**, *19*, 3182. [CrossRef] [PubMed]
14. Garcia, C.; Furtado de Almeida, A.A.; Costa, M.; Britto, D.; Valle, R.; Royaert, S.; Marelli, J.P. Abnormalities in somatic embryogenesis caused by 2.4-D: An overview. *Plant Cell Tissue Organ Cult.* **2019**, *137*, 193–212. [CrossRef]
15. Abrahamsson, M.; Valladares, S.; Larsson, E.; Clapham, D.; Von Arnold, S. Patterning during somatic embryogenesis in Scots pine in relation to polar auxin transport and programmed cell death. *Plant Cell Tissue Organ Cult.* **2012**, *109*, 391–400. [CrossRef]
16. Breton, D.; Harvengt, L.; Trontin, J.F.; Bouvet, A.; Favre, J.M. High subculture frequency, maltose-based and hormone-free medium sustained early development of somatic embryos in maritime pine. *Vitr. Cell. Dev. Biol. Plant* **2005**, *41*, 494–504. [CrossRef]

17. Klimaszewska, K.; Noceda, C.; Pelletier, G.; Label, P.; Rodriguez, R.; Lelu-Walter, M.A. Biological Characterization of Young and Aged Embryogenic Cultures of *Pinus pinaster* (Ait.). *Vitr. Cell. Dev. Biol. Plant* **2009**, *45*, 20–33. Available online: http://www.jstor.org/stable/20540999 (accessed on 8 June 2023).
18. Sun, T.; Wang, Y.; Zhu, L.; Liu, X.; Wang, Q.; Ye, J. Evaluation of somatic embryo production during embryogenic tissue proliferation stage using morphology, maternal genotype, proliferation rate and tissue age of *Pinus thunbergia* Parl. *J. For. Res.* **2022**, *33*, 445–454. [CrossRef]
19. Peng, C.; Gao, F.; Wang, H.; Shen, H.; Yang, L. Optimization of maturation process for somatic embryo production and cryopreservation of embryogenic tissue in *Pinus koraiensis*. *Plant Cell Tissue Organ Cult.* **2021**, *144*, 185–194. [CrossRef]
20. Ree, J.F.; Polesi, L.G.; Back, F.; Azevedo-Bertolazi, A.; Silveira, V.; Guerra, M.P. Aging peach palm (*Bactris gasipaes* Kunth) cultures lose embryogenic potential and metabolic cellular function due to continuous culture in hypoxic environments. *Plant Cell Tissue Organ Cult.* **2020**, *140*, 49–67. [CrossRef]
21. Breton, D.; Harvengt, L.; Trontin, J.F.; Bouvet, A.; Favre, J.M. Long-term subculture randomly affects morphology and subsequent maturation of early somatic embryos in maritime pine. *Plant Cell Tissue Organ Cult.* **2006**, *87*, 95–108. [CrossRef]
22. Egertsdotter, U. Plant physiological and genetical aspects of the somatic embryogenesis process in conifers. *Scand. J. For. Res.* **2019**, *34*, 360–369. [CrossRef]
23. Filonova, L.H.; Bozhkov, P.V.; Brukhin, V.B.; Daniel, G.; Zhivotovsky, B.; Von Arnold, S. Two waves of programmed cell death occur during formation and development of somatic embryos in the gymnosperm, Norway spruce. *J. Cell Sci.* **2000**, *24*, 4399–4411. [CrossRef]
24. Ávila, C.; Llebrés, M.T.; Castro-Rodríguez, V.; Lobato-Fernández, C.; Reymond, I.; Harvengt, L.; Trontin, J.F.; Cánovas, F.M. Identification of Metabolic Pathways Differentially Regulated in Somatic and Zygotic Embryos of Maritime Pine. *Front. Plant Sci.* **2022**, *13*, 877960. [CrossRef]
25. Passamani, L.Z.; Reis, R.S.; Vale, E.M.; Sousa, K.R.; Aragão, V.P.M.; Santa-Catarina, C.; Silveira, V. Long-term culture with 2.4-dichlorophenoxyacetic acid affects embryogenic competence in sugarcane callus via changes in starch, polyamine and protein profiles. *Plant Cell Tissue Organ Cult.* **2020**, *140*, 415–429. [CrossRef]
26. Dowlatabadi, R.; Weljie, A.M.; Thorpe, T.A.; Yeung, E.C.; Vogel, H.J. Metabolic footprinting study of white spruce somatic embryogenesis using NMR spectroscopy. *Plant Physiol. Biochem.* **2009**, *47*, 343–350. [CrossRef] [PubMed]
27. do Nascimento, A.M.M.; Polesi, L.G.; Back, F.P.; Steiner, N.; Guerra, M.P.; Castander-Olarieta, A.; Moncaleán, P.; Montalbán, I.A. The Chemical Environment at Maturation Stage in *Pinus* spp. Somatic Embryogenesis: Implications in the Polyamine Profile of Somatic Embryos and Morphological Characteristics of the Developed Plantlets. *Front. Plant Sci.* **2019**, *12*, 771464. [CrossRef]
28. Rodrigues, A.S.; De Vega, J.J.; Miguel, C.M. Comprehensive assembly and analysis of the transcriptome of maritime pine developing embryos. *BMC Plant Biol.* **2018**, *18*, 379. [CrossRef] [PubMed]
29. Castander-Olarieta, A.; Pereira, C.; Montalbán, I.A.; Mendes, V.M.; Correia, S.; Suárez-Álvarez, S.; Manadas, B.; Canhoto, J.; Moncaleán, P. Proteome-Wide Analysis of Heat-Stress in *Pinus radiata* Somatic Embryos Reveals a Combined Response of Sugar Metabolism and Translational Regulation Mechanisms. *Front. Plant Sci.* **2021**, *12*, 631239. [CrossRef]
30. Arrillaga, I.; Morcillo, M.; Zanón, I.; Lario, F.; Segura, J.; Sales, E. New Approaches to Optimize Somatic Embryogenesis in Maritime Pine. *Front. Plant Sci.* **2019**, *10*, 138. [CrossRef] [PubMed]
31. Han, Y.; Han, L.; Yao, Y.; Li, Y.; Liu, X. Key factors in FTIR spectroscopic analysis of DNA: The sampling technique, pretreatment temperature and sample concentration. *Anal. Methods* **2018**, *10*, 436–2443. [CrossRef]
32. Naseer, K.; Ali, S.; Qazi, J. ATR-FTIR spectroscopy as the future of diagnostics: A systematic review of the approach using bio-fluids. *Appl. Spectrosc. Rev.* **2021**, *56*, 85–97. [CrossRef]
33. Bansal, A.; Kaushik, S.; Kukreti, S. Non-canonical DNA structures: Diversity and disease association. *Front. Genet.* **2022**, *13*, 959258. [CrossRef]
34. Dong, L.; Duan, X.; Bin, L.; Wang, J.; Gao, Q.; Sun, X.; Xu, Y. Evaluation of Fourier transform infrared (FTIR) spectroscopy with multivariate analysis as a novel diagnostic tool for lymph node metastasis in gastric cancer. *Spectrochim. Acta A Mol. Biomol. Spectrosc.* **2023**, *289*, 122209. [CrossRef] [PubMed]
35. Pereira de Souza, N.M.; Machado, B.H.; Padoin, L.V.; Prá, D.; Fay, A.P.; Corbellini, V.A.; Rieger, A. Rapid and low-cost liquid biopsy with ATR-FTIR spectroscopy to discriminate the molecular subtypes of breast cancer. *Talanta* **2023**, *254*, 123858. [CrossRef] [PubMed]
36. Bravo, S.; Bertín, A.; Turner, A.; Sepulveda, F.; Jopia, P.; Parra, M.J.; Castillo, R.; Hasbún, R. Differences in DNA methylation, DNA structure and embryogenesis-related gene expression between embryogenic and non embryogenic lines of *Pinus radiata* D. don. *Plant Cell Tissue Organ Cult.* **2017**, *130*, 521–529. [CrossRef]
37. Litvay, J.; Verma, D.; Johnson, M. Influence of a loblolly pine (*Pinus taeda* L.). Culture medium and its components on growth and somatic embryogenesis of the wild carrot (*Daucus carota* L.). *Plant Cell Rep.* **1985**, *4*, 325–328. [CrossRef] [PubMed]
38. Hargreaves, C.; Grace, L.; Holden, D. Nurse culture for efficient recovery of cryopreserved *Pinus radiata* D. Don embryogenic cell lines. *Plant Cell Rep.* **2002**, *21*, 40–45. [CrossRef]
39. Pullman, G.S.; Johnson, S.; Peter, G.; Cairney, J.; Xu, N. Improving loblolly pine somatic embryo maturation: Comparison of somatic and zygotic embryo morphology, germination, and gene expression. *Plant Cell Rep.* **2003**, *21*, 747–758. [CrossRef]
40. Brereton, R.G.; Lloyd, G.R. Partial least squares discriminant analysis: Taking the magic away. *J. Chemom.* **2014**, *28*, 213–225. [CrossRef]
41. Fordellone, M.; Bellincontro, A.; Mencarelli, F. Partial least squares discriminant analysis: A dimensionality reduction method to classify hyperspectral data. *Stat. Appl. Ital. J. Appl. Stat.* **2020**, *31*, 181–200. [CrossRef]

42. Ruiz-Perez, D.; Guan, H.; Madhivanan, P.; Mathee, K.; Narasimhan, G. So you think you can PLS-DA? *BMC Bioinform.* **2020**, *21*, 2. [CrossRef]
43. Ding, C.; Park, Y.S.; Bonga, J.; Bartlett, B.; Li, Y.; Raley, F. A brief review of combining genomic selection and somatic embryogenesis for tree improvement. In Proceedings of the 5th International Conference of the IUFRO Working Party 2.09.02 "Clonal Trees Bioeconomy Age: Opportunities and Challenges", Coimbra, Portugal, 10–15 September 2018.
44. Calleja-Rodríguez, A.; Klápště, J.; Dungey, H.; Graham, N.; Ismael, A.; García-Gil, M.R.; Abrahamsson, S.; Suontama, M. Genomic Selection in Scots (*Pinus Sylvestris*) and Radiata (*Pinus Radiata*) Pines. In *The Pine Genomes*; De La Torre, A.R., Ed.; Compendium of Plant Genomes; Springer: Cham, Switzerland, 2022; pp. 233–250. [CrossRef]
45. Bonga, J.; Park, Y.S.; Ding, C. What technical improvements are needed to achieve industrial application of conifer somatic embryogenesis? In Proceedings of the 5th International Conference of the IUFRO Working Party 2.09.02 "Clonal Trees Bioeconomy Age: Opportunities and Challenges", Coimbra, Portugal, 10–15 September 2018.
46. Zhu, T.; Wang, J.; Hu, J.; Ling, J. Mini review: Application of the somatic embryogenesis technique in conifer species. *For. Res.* **2022**, *2*, 18. [CrossRef]
47. Nielsen, U.B.; Hansen, C.B.; Hansen, U.; Johansen, V.K.; Egertsdotter, U. Accumulated effects of factors determining plant development from somatic embryos of *Abies nordmanniana* and *Abies bornmuelleriana*. *Front. Plant Sci.* **2022**, *13*, 989484. [CrossRef]
48. Xia, X.R.; Yang, F.; Ke, X.; Chen, Y.M.; Ye, J.R.; Zhu, L.H. Somatic embryogenesis of masson pine (*Pinus massoniana*): Initiation, maturation and genetic stability analysis at SSR loci. *Plant Cell Tissue Organ Cult.* **2021**, *145*, 667–677. [CrossRef]
49. Li, Q.; Deng, C.; Zhu, T.; Ling, J.; Zhang, H.; Kong, L.; Zhang, S.; Wang, J.; Chen, X. Dynamics of physiological and miRNA changes after long-term proliferation in somatic embryogenesis of *Picea balfouriana*. *Trees* **2019**, *33*, 469–480. [CrossRef]
50. Salaj, T.; Klubicová, K.; Panis, B.; Swennen, R.; Salaj, J. Physiological and Structural Aspects of In Vitro Somatic Embryogenesis in *Abies alba* Mill. *Forests* **2020**, *11*, 1210. [CrossRef]
51. Brunoni, F.; Collani, S.; Casanova-Sáez, R.; Šimura, J.; Karady, M.; Schmid, M.; Ljung, K.; Bellini, C. Conifers exhibit a characteristic inactivation of auxin to maintain tissue homeostasis. *N. Phytol.* **2020**, *226*, 1753–1765. [CrossRef]
52. Liang, Y.; Xu, X.; Shen, H.; Gao, M.; Zhao, Y.; Bai, X. Morphological and endogenous phytohormone changes during long-term embryogenic cultures in Korean pine. *Plant Cell Tissue Organ Cult.* **2022**, *151*, 253–264. [CrossRef]
53. Llebrés, M.T.; Pascual, M.B.; Debille, S.; Trontin, J.F.; Harvengt, L.; Avila, C.; Cánovas, F.M. The role of arginine metabolic pathway during embryogenesis and germination in maritime pine *(Pinus pinaster* Ait.). *Tree Physiol.* **2018**, *38*, 471–484. [CrossRef]
54. Maruyama, T.E.; Hosoi, Y. Progress in Somatic Embryogenesis of Japanese Pines. *Front. Plant Sci.* **2019**, *10*, 31. [CrossRef]
55. Dunstan, D.I.; Bethune, T.D. Variability in Maturation and Germination from White Spruce Somatic Embryos, as Affected by Age and Use of Solid or Liquid Culture. *Vitr. Cell. Dev. Biol. Plant* **1996**, *32*, 165–170. Available online: http://www.jstor.org/stable/20064900 (accessed on 8 June 2023). [CrossRef]
56. Bobadilla Landey, R.; Cenci, A.; Guyot, R.; Bertrand, B.; Georget, F.; Dechamp, E.; Herrera, J.C.; Aribi, J.; Lashermes, P.; Etienne, H. Assessment of genetic and epigenetic changes during cell culture ageing and relations with somaclonal variation in *Coffea arabica*. *Plant Cell Tissue Organ Cult.* **2015**, *122*, 517–531. [CrossRef]
57. Bradaï, F.; Pliego-Alfaro, F.; Sánchez-Romero, C. Long-term somatic embryogenesis in olive (*Olea Europaea*): Influence on regeneration capability and quality of regenerated plants. *Sci. Hortic.* **2016**, *199*, 23–31. [CrossRef]
58. Gao, Y.; Cui, Y.; Zhao, R.; Chen, X.; Zhang, J.; Zhao, J.; Kong, L. Cryo-Treatment Enhances the Embryogenicity of Mature Somatic Embryos via the lncRNA–miRNA– mRNA Network in White Spruce. *Int. J. Mol. Sci.* **2022**, *23*, 1111. [CrossRef] [PubMed]
59. Carneros, E.; Hernández, I.; Toribio, M.; Díaz-Sala, C.; Celestino, C. Effect of different cryoprotectant procedures on the recovery and maturation ability of cryopreserved *Pinus pinea* embryogenic lines of different ages. *Vitr. Cell. Dev. Biol. Plant* **2017**, *53*, 469–477. [CrossRef]
60. Tikkinen, M.; Varis, S.; Aronen, T. Development of Somatic Embryo Maturation and Growing Techniques of Norway Spruce Emblings towards Large-Scale Field Testing. *Forests* **2018**, *9*, 325. [CrossRef]
61. Etienne, H.; Bertrand, B. Somaclonal variation in *Coffea arabica*: Effects of genotype and embryogenic cell suspension age on frequency and phenotype of variants. *Tree Physiol.* **2003**, *23*, 419–426. [CrossRef] [PubMed]
62. Goryachkina, O.V.; Park, M.E.; Tretyakova, I.N.; Badaeva, E.D.; Muratova, E.N. Cytogenetic stability of young and long-term embryogenic cultures of *Larix sibirica*. *Cytologia* **2018**, *83*, 323–329. [CrossRef]
63. Marum, L.; Loureiro, J.; Rodriguez, E.; Santos, C.; Oliveira, M.M.; Miguel, C. Flow cytometric and morphological analyses of *Pinus pinaster* somatic embryogenesis. *J. Biotechnol.* **2009**, *143*, 288–295. [CrossRef]
64. Pila Quinga, L.A.; Pacheco de Freitas Fraga, H.; do Nascimento Vieira, L.; Guerra, M.P. Epigenetics of long-term somatic embryogenesis in *Theobroma cacao* L.: DNA methylation and recovery of embryogenic potential. *Plant Cell Tissue Organ Cult.* **2017**, *131*, 295–305. [CrossRef]
65. Noceda, C.; Salaj, T.; Pérez, M.; Viejo, M.; Cañal, M.J.; Salaj, J.; Rodriguez, R. DNA demethylation and decrease on free polyamines is associated with the embryogenic capacity of *Pinus nigra* Arn. cell culture. *Trees* **2009**, *23*, 1285–1293. [CrossRef]
66. Tymchenko, E.E.; Soldatova, A.A.; Chikhirzhina, E.V.; Polyanichko, M. Analysis of Changes in the Structure of DNA when Interacting with Platinum Coordination Compounds by IR Spectroscopy. *Biophysics* **2022**, *67*, 15–21. [CrossRef]
67. Mello, M.L.S.; Vidal, B.C. Changes in the Infrared Microspectroscopic Characteristics of DNA Caused by Cationic Elements, Different Base Richness and Single-Stranded Form. *PLoS ONE* **2012**, *7*, e43169. [CrossRef] [PubMed]

68. Tymchenko, E.; Glova, A.; Soldatova, A.; Chikhirzhina, E.; Polyanichko, A. FTIR Study of the Secondary Structure of DNA in Complexes with Platinum Coordination Compounds. *J. Phys. Conf.* **2019**, *1400*, 033004. [CrossRef]
69. Serec, K.; Šegedin, N.; Krajacic, M.; Babić, S. Conformational Transitions of Double-Stranded DNA in Thin Films. *Appl. Sci.* **2021**, *11*, 2360. [CrossRef]
70. Fabian, H.; Jackson, M.; Murphy, L.; Watson, P.H.; Fichtner, I.; Mantsch, H.H. A comparative infrared spectroscopic study of human breast tumors and breast tumor cell xenografts. *Biospectroscopy* **1995**, *1*, 37–45. [CrossRef]
71. Sofińska, K.; Wilkosz, N.; Szymoński, M.; Lipiec, E. Molecular Spectroscopic Markers of DNA Damage. *Molecules* **2020**, *25*, 561. [CrossRef]
72. Banyay, M.; Sarkar, M.; Gräslund, A. A library of IR bands of nucleic acids in solution. *Biophys. Chem.* **2003**, *104*, 477–488. [CrossRef]
73. Geinguenaud, F.; Militello, V.; Arluison, V. Application of FTIR Spectroscopy to Analyze RNA Structure. In *RNA Spectroscopy. Methods in Molecular Biology*; Arluison, V., Wien, F., Eds.; Humana: New York, NY, USA, 2020; Volume 2113, pp. 119–133. [CrossRef]
74. Dovbeshko, G.I.; Gridina, N.Y.; Kruglova, E.B.; Pashchuk, O.P. FTIR spectroscopy studies of nucleic acid damage. *Talanta* **2000**, *53*, 233–246. [CrossRef]